GSI-ESA-NASA Nuclear Cross-Section Database: Update I. Addition of Proton-Projectile Reaction Cross-Sections

Francesca Luoni¹, Reka Szabo^{2,3}, Daria Boscolo², Charles Werneth⁴

Abstract: Nuclear reaction cross-sections are needed for Monte Carlo and deterministic radiation transport codes used for ion therapy and radiation protection in space. A GSI-ESA-NASA combined effort generated a free and publicly-available nucleus-nucleus reaction cross-section database. Nevertheless, protons—the main component of solar particle events and galactic cosmic ray fluences in space—account alone for over 60% of the effective dose behind thick shields in space and are used in 88% of the cancer-treatment ion-therapy centers worldwide. Therefore, in the present work, proton-projectile data have also been included. These data are compared to the reaction cross-section models used in radiation transport codes, including the models of Tripathi-Cucinotta-Wilson, Hybrid-Kurotama, Kox, Shen, and Kox-Shen. The Tripathi-Cucinotta-Wilson model uses the Tripathi99 model for low-Z projectile ions and the Tripathi96 model for other projectiles. The Hybrid-Kurotama model is based on the Black Sphere formula at high energies that is smoothly connected to the Tripathi99 model at low energies. It is found that the Tripathi99 and Hybrid-Kurotama models best fit the proton-projectile data.

Keywords: space exploration, radiation protection in space, shielding in space, ion therapy, nuclear reaction cross-sections, proton-projectile cross-sections

¹ Analytical Mechanics Associates, Hampton, VA (US)

² GSI Helmholtz Center for Heavy-Ion Research, Darmstadt (Germany)

³ Budapest University of Technology and Economics (Hungary)

⁴ NASA Langley Research Center, Hampton, VA (US)

1. Introduction

Human spaceflight is expected to flourish in the future with missions beyond low-Earth orbit including the Moon, Mars, and deep space. Among the many human health hazards associated with spaceflight are the low-gravity environment, isolation and confinement, distance from Earth, hostile environment, and space radiation (Afshinneko et al. (2020)). Space radiation is a complex mixture of high linear-energy-transfer (LET) radiation that arises from Solar Energetic Particles (SEPs) and Galactic Cosmic Rays (GCRs). SEPs are mostly composed of protons with energies that reach several hundred MeV and higher, whereas GCRs are composed of mostly protons and heavier nuclei with energies that reach TeV/u and higher (Benton and Benton (2001)). All but the most energetic SEPs are mitigated with passive shielding employed in spacecraft (National Research Council (2008), Washburn et al. (2015), Slaba et al. (2017)) while higher energy GCRs penetrate deeply into the vehicle and human tissue and represent a significant shielding challenge for space agencies and crewmembers (Luoni et al. (2022)).

In addition to space applications, ion radiation in the energy range of tens to a few hundred MeV/u is widely used in ion therapy. These two fields share many similarities (Tinganelli et al. (2021)). Particle therapy has emerged as a highly effective cancer treatment. Charged nuclei exhibit a favorable depth-dose distribution in the human body due to the Bragg peak, allowing for precise radiation delivery to tumors while minimizing exposure to healthy tissues compared to conventional radiotherapy (Durante and Haberer (2024)). This rapidly expanding field is growing worldwide, with 124 proton therapy centers and 17 carbon-ion therapy centers currently in operation, and many more in the planning and construction phases⁵.

Protons are crucial in both the fields of radiation protection in space and ion therapy. Protons are a major concern for space radiation exploration because of their large relative abundance. GCRs consist of approximately 2% electrons and 98% baryons, where the baryonic component comprises 85% protons, 14% helium nuclei, and 1% heavier ions (Chancellor et al. (2014)). Protons are produced copiously in solar particle events and are the main contributor to trapped particle radiation exposure for crew members during low-Earth orbit missions. Behind thick shielding configurations, such as the International Space Station (approximately 2-1000 g/cm², Koontz et al. (2005), Slaba et al. (2013)) and spacecraft that may be used for near-future Moon and Mars missions, protons and helium ions become the most relevant for dose and dose equivalent contributions (Norbury et al. (2020)). In particular, it was calculated that, behind a 20 g/cm² aluminium shield, 68% of the total effective dose is due to protons (Slaba and Blattnig (2014)). This number increases to 70% behind a 40 g/cm²

_

⁵ ptcog.site/index.php/facilities-in-operation-publication

aluminium shield. These predictions are also supported by Geant4 calculations (Norbury et al. (2020)).

The importance of proton nuclear interactions in therapy mirrors the rationale for space radiation protection. In carbon-ion therapy, protons are the most abundant secondary projectiles produced during projectile fragmentation processes. These protons contribute to both the lateral and longitudinal spread of the beam, particularly in the tail region beyond the Bragg peak. Therefore, their contribution to the final dose and radiobiological effects must be carefully considered in beam transport calculations as well as in treatment planning and optimization (Durante and Paganetti (2016)). In contrast, proton therapy primarily involves target fragmentation, predominantly generating secondary protons and neutrons. These target fragments, typically low in energy and thus high in LET, contribute to a fragmentation-induced buildup effect in the proton beam entrance channel. While their impact on physical dose and primary proton beam attenuation is already included in treatment planning softwares, recent studies suggest that more accurate descriptions of their production yields and energy spectra within the relevant energy range could enhance radiobiological dose estimations, particularly in the entrance channel (Bellinzona et al. (2021)).

Reliable radiation transport codes are used for risk assessment tools; space radiation shielding design; and optimization and safety of ion therapy. The particle fluences produced from the radiation transport codes require validated nuclear cross-section models (Townsend et al. (2002), Norbury et al. (2012), Luoni (2023a)) that are essential for providing the mean free paths for the interactions of GCR and SEP radiation with passive shielding in spacecraft and human tissues, and therapeutic ion beam interactions with passive modulators in clinical applications. Many radiation transport codes exist and are also used for other endpoints, spanning from particle accelerator research, to particle, nuclear physics, and astrophysics applications (Norbury et al. (2012)).

Several studies (Slaba et al. (2020), Luoni et al. (2022), Luoni et al. (2025)) that compared the doses of various Monte Carlo and deterministic radiation transport codes reveal that differences in the results are largely due to the variation of the nuclear cross-section models utilized. Consequently, nuclear cross section databases are essential for determining the veracity of the cross-section models to ensure particle doses are accurate.

In a previous study, a cross section database for nucleus-nucleus reactions was assembled through combined effort of GSI (Gesellschaft fuer Schwerionenforschung—Society for Heavy-Ion Research), ESA (European Space Agency), and NASA (National Aeronautics and Space Administration) (Luoni et al. (2021)). This database augmented a previous work (Norbury et al. (2011), Norbury et al. (2012)) and is accessible online from from the GSI website⁶. Additionally, the experimentally measured data collected in the database were used to benchmark the reaction cross-section models used in radiation transport codes. The models are: Tripathi-Cucinotta-

_

⁶ https://www.gsi.de/fragmentation

Wilson, Kox, Shen, Kox–Shen, and Hybrid-Kurotama. An optimization of the Tripathi-Cucinotta-Wilson model was proposed (Luoni et al. (2023b)) to fit experimental data more accurately than the legacy models studied. The impact of this optimization on the Hybrid-Kurotama model was also evaluated, as it makes use of the Tripathi-Cucinotta-Wilson model at low energies.

The present work focuses on updating the nuclear reaction cross section database to include proton-nucleus reactions thefore providing additional opportunity for the assessment of nuclear model accuracy.

2. Addition of Proton-Projectile Data to the GSI-ESA-NASA Nuclear Reaction Cross-Section Database

As explained in Section 1, proton-projectile data are crucial in both the fields of radiation protection in space and ion therapy. Therefore, proton-projectile data have been added to the GSI-ESA-NASA reaction cross-section database.

Within the scope of this work, 1008 total reaction cross-section proton-projectile data were added to the original database from 53 publications (Cassels and Lawson (1954), Millburn et al. (1954), Chen et al. (1955), Burge (1959), Gooding (1959), Meyer and Carlson (1960a), Meyer and Hintz (1960b), Albert and Hansen (1961), Greenlees and Jarvis (1961), Johansson et al. (1961), Carlson et al. (1962), Goloskie and Strauch (1962), Wilkins and Igo (1963), Giles and Burge (1964), Makino et al. (1964), Turner et al. (1964), Bearpark (1965), Bulman et al. (1965), Dell et al. (1965), Makino et al. (1965a), Makino et al. (1965b), Pollock and Schrank (1965), Kirkby and Link (1966), Chapman and Macleod (1967), Dicello et al. (1967), Bulman and Griffith (1968), Hojvat and Jones (1968), Dicello and Igo (1970), Menet et al. (1971), Bertini (1972), Nicholls et al. (1972), Renberg et al. (1972), Bertrand and Peelle (1973), Montague et al. (1973), McGill et al. (1974), Carlson et al. (1975), Slaus et al. (1975), Sourkes et al. (1976), Davison et al. (1977), Jaros et al. (1978), Nasr et al. (1978), Abegg et al. (1979), Anderson et al. (1979), Segel et al. (1982), McGill et al. (1984), Carlson et al. (1985), McCamis et al. (1986), Carlson et al. (1994), Singh et al. (1994), Carlson et al. (1995), Eliyakut-Roshko et al. (1995), Carlson (1996), Enke et al. (1999)).

The original database had 1786 cross-section data from 103 publications (Luoni et al. (2021) and references within). Consequently, the database now contains 2794 data points from 156 publications. The publication criteria are the same as for the original database (Luoni et al. (2021)).

In the database, the experimental error bars were taken from the original publications. Some authors only report statistical errors, some also systematic uncertainties, in which case a combination of the two was evaluated (Luoni et al. (2021)). The error type was specified in the database for each data point. If multiple measurements were performed with the same experimental setup, the average cross-section was

calculated, and its uncertainty was derived by propagating statistical and systematic errors.

Fig. 1 reports the number of reaction cross-section data points included in the GSI-ESA-NASA cross-section database as a function of the projectile atomic number, Z_p , before and after the addition of proton-projectile data points. Reaction cross-sections refer to the probability that a non-elastic nuclear reaction will occur. Charge-changing cross-sections refer to the probability for the projectile nucleus to undergo a nuclear reaction that changes its atomic number. Therefore, reactions that change only its mass number e.g., neutron stripping, are a subgroup of reaction cross-sections, but not of charge-changing cross-sections (Luoni et al. (2021)). Fig. 1 is limited to projectiles up to nickel where thereafter particle fluences in the space radiation environment contribute negligibly to dose; likewise, nuclei with masses greater than nickel have not been used frequently for radiation therapy. The data referring to Z_p =1 before the addition of proton-projectile data, are mostly for deuteron-projectiles. Proton-projectle data are more abundant than any other projectile (Szabo (2023)). All proton-projectile data in this database are composed of reaction cross-sections (green in Fig. 1b).

In Fig. 2, the proton-projectile reaction cross-section entry numbers are shown as a function of the atomic number of the target nuclei. Specific targets are useful for endpoints spanning from nuclear engineering to nuclear physics, planetary physics, and astrophysics.

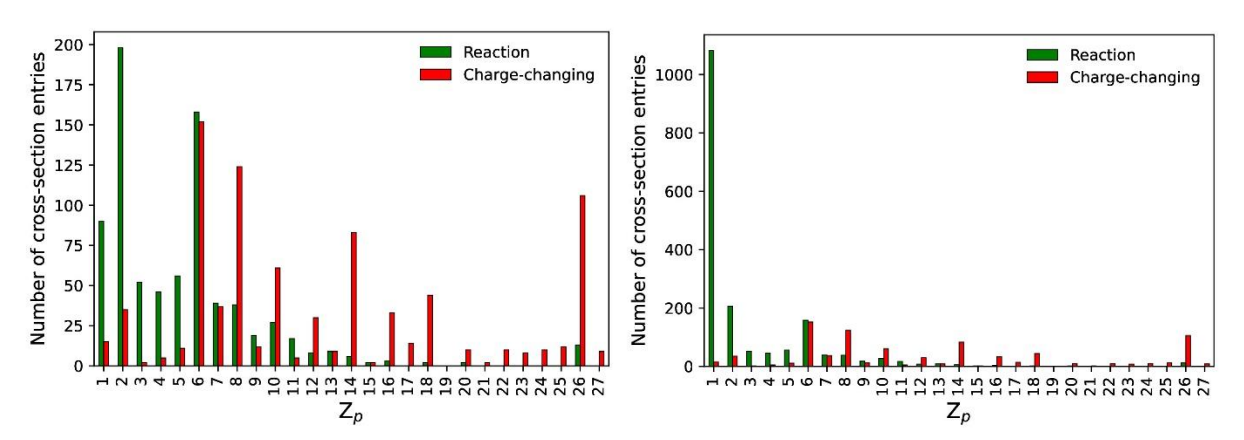


Figure 1: Number of cross-section data points in the reaction cross-section database as a function of the atomic number of the projectile nucleus, Z_p , before (Fig. 1a) and after (Fig. 1b) the addition of proton data. Charge-changing cross-section entry numbers are shown in red and reaction cross-sections are in green. Entries up to nickel projectiles only are reported.

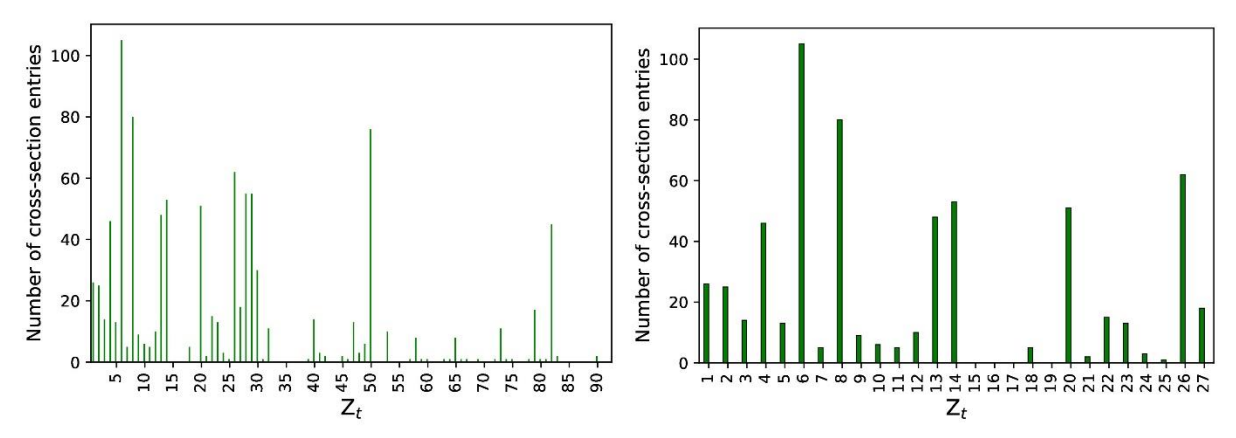


Figure 2: Number of proton-projectile reaction cross-section data added to the database as a function of the target atomic number. Fig. 2a shows all targets used for proton-projectile measurements. Figure 2b is a closed-up view on targets up to nickel, which correspond to the data of interest for space and therapy applications.

3. Comparison of the Collected Data with the Models Used for Radiation Transport Codes

The target nuclei of primary interest for space are as follows: ¹H, ⁷Li, ¹²C, ¹⁶O, ²⁷Al, and ²⁸Si (Luoni et al. (2022)). ¹H, ¹²C, and ¹⁶O are the main constituents of the human body, and ²⁷Al is utilized as spacecraft structural material. Electronic instrumentation comprises ²⁸Si, and SiO₂ is the main constituent of Moon and Mars regolith, which can be used as *in situ* additional shielding. Lithium-based hydrides, mainly composed of ¹H and ⁷Li are potential innovative shielding materials that have been tested through simulations and experiments. ¹H and ¹²C are the main components of the well-established shielding material polyethylene. Finally, H₂O is a so-called dual-use shielding material to be used during the interplanetary flights.

The target nuclei of primary interest for ion-therapy are: ¹H, ¹²C, and ¹⁶O, since they are the main contituents of the human body. ¹H, ¹²C, and ¹⁶O are also common in materials composing passive modulators, which are positioned between the particle beam and the patient (Mohan and Grosshans (2017)).

Since ¹H is also an important target nucleus, proton-projectile cross-section data can also be used to evaluate inverse kinematic (IK) cross-sections of other ions reacting with proton-targets. The IK notation means that the projectile and target frames are reversed. Reaction cross-sections are conserved when the same kinetic energy per nucleon of the projectile and target are used after transforming frames (Norbury et al. (2011)). For instance, the total reaction cross-section of a 500 MeV proton (projectile) impinging on a ¹²C (target) is the same as the total reaction cross-section of a 500 MeV/u ¹²C (projectile) on an ¹H (target).

As done for nucleus-nucleus cross-section data (Luoni et al. (2021)), in this work, the experimentally measured data collected in the database are used to benchmark reaction cross-section models employed in radiation transport codes: the Tripathi-Cucinotta-Wilson (Tripathi et al. (1996), Tripathi et al. (1999)), Kox (Kox et al. (1987)), Shen (Shen et al. (1989)), Kox–Shen (Sihver et al. (2014b)), and Hybrid-Kurotama (Sihver et al. (2014a)) models. The Hybrid-Kurotama model is based on the Black Sphere (Kurotama, in Japanese) formula, smoothly connected to the Triapthi-Cucinotta-Wilson parameterization at low energies.

The Kox, Shen, and Tripathi-Cucinotta-Wilson models are implemented in Geant4 (Agostinelli et al. (2003), Allison et al. (2016)), even though none of them is used by default within any of the Geant4 physics lists. Hybrid-Kurotama is the default model for PHITS⁷ (Kox–Shen and Tripathi-Cucinotta-Wilson are options). FLUKA (Battistoni et al. (2015), Hugo et al. (2024)), the NASA HZETRN (Slaba et al. (2020)), and the GSI in-house heavy-ion treatment planning system TRiP98 (Kraemer et al. (2000)) codes use the Tripathi-Cucinotta-Wilson model.

Fig. 3 reports proton-projectile data points collected for ⁷Li, ¹²C, ¹⁶O, ²⁷Al, and ²⁸Si targets, in direct and IK. The predictions of the Kox-Shen semi-empirical model are added to guide the reader's eyes through the data.

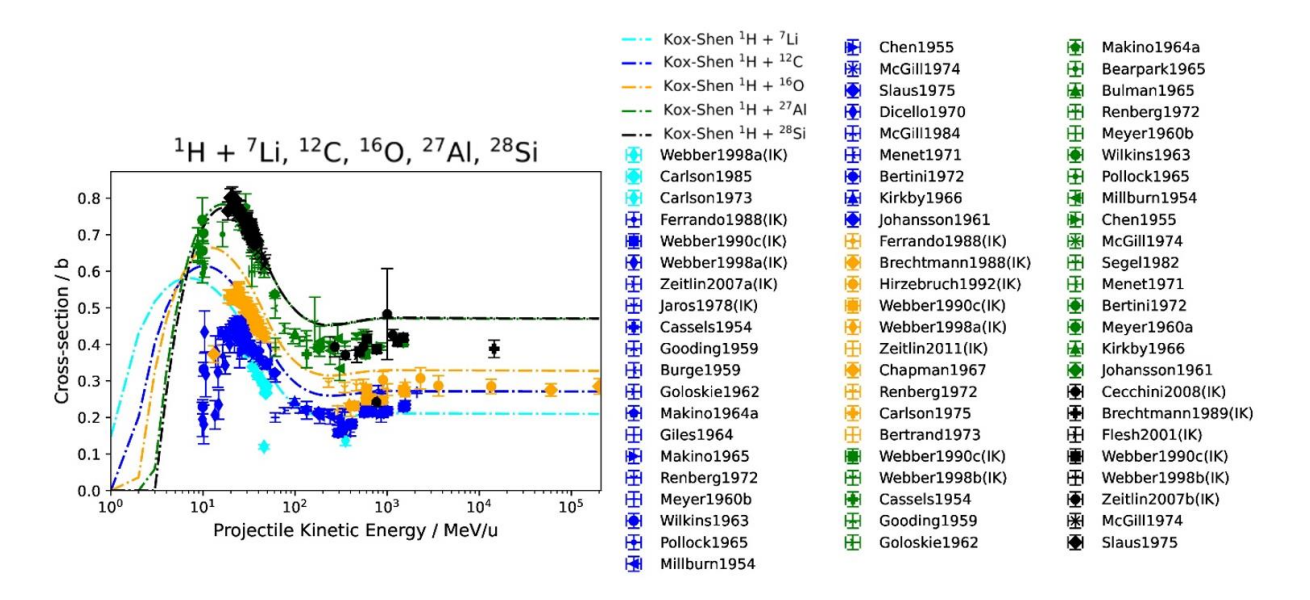


Figure 3: Data collection for proton projectiles on different targets, alongside the predictions of the Kox-Shen semi-empirical model. IK stands for inverse kinematic data. Different colours represent different targets. Both reaction and charge-changing cross-sections are plotted. The references from which the data were collected are reported in the legend.

_

⁷ https://phits.jaea.go.jp/manual/manualE-phits.pdf

In Fig. 4 to 8, proton reaction cross-section data are plotted as a function of the projectile kinetic energy. The predictions of the aforementioned cross-section models are plotted alongside the data. For each set of figures, the subfigure on the left represents the data collection before the addition of proton-projectile data (Luoni et al. (2021)). As a consequence, the experimental data points in the subfigures on the left were all measured in IK. The subfigure on the right also contains the proton-projectile data collected in the scope of this work.

The system ¹H + ⁴He is presented in Fig. 4 because of its importance in IK, as ⁴He is a main contributor to dose equivalent in space behind thick shields (Norbury et al. (2020), Luoni et al. (2025)). For ¹H + ⁷Li (Fig. 5), one data point (Carlson et al. (1973)) appears not to agree with the data from the other dataset (Carlson et al. (1985)).

The Tripathi99 model refers to the Tripathi96 model adapted to light nuclei such as protons. The Hybrid-Kurotama model follows the Tripathi99 model until a threshold energy value is reached. Therefore, the two models are superimposed at low energies. For ¹H + ⁴He (Fig. 4), ¹H + ⁷Li (Fig. 5), and ¹H + ¹²C (Fig. 6), the Tripathi96 and Tripathi99 differ greatly at low energies. This difference becomes smaller for ¹H + ²⁷Al (Fig. 7) and ¹H + ⁵⁶Fe (Fig. 8). The Hybrid-Kurotama model follows the trend of Tripathi99 at low energies.

For ¹H + ⁴He, the Tripathi99 and Hybrid-Kurotama models fit the low-energy data (Sourkes et al. (1976)) well. Data measured by different authors for ¹H + ⁷Li and ¹H + ¹²C suggest that the Kox, Shen and Kox-Shen models yield cross-section predictions that are too large at the energies that correspond to the peak of the curve (10 to 30 MeV/u). For higher-Z targets, the discrepancies between models are not as large; due to the scattering of data from the different datasets, no clear conclusion about which models fit the data better can be drawn.

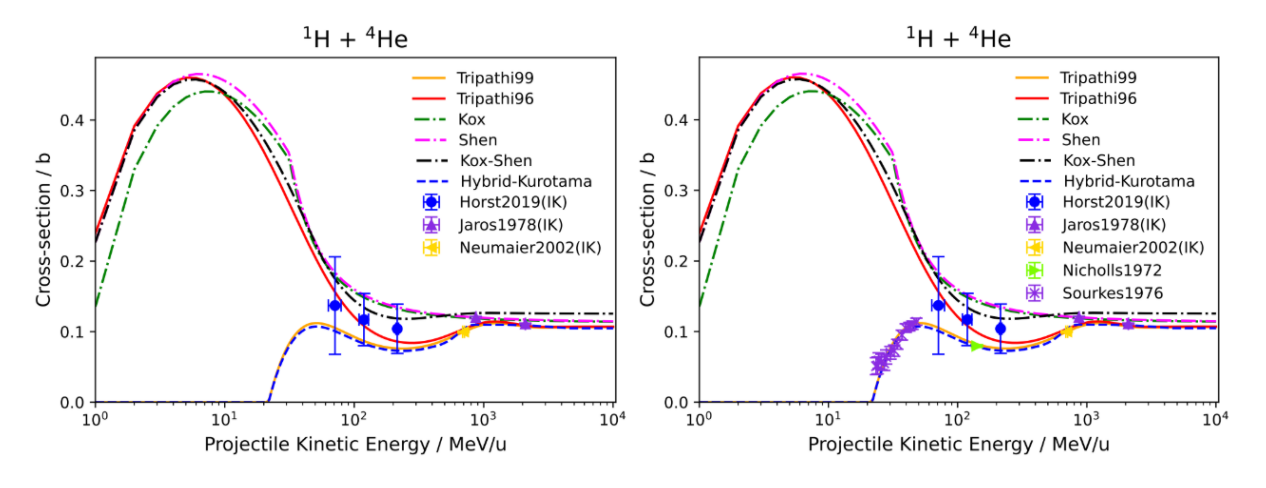


Figure 4: Comparison between models results and cross-section data for proton projectiles on ⁴He targets, before (Fig. 4a) and after (Fig. 4b) the addition to the database of proton-projectile data presented in this work. IK stands for inverse kinematic data.

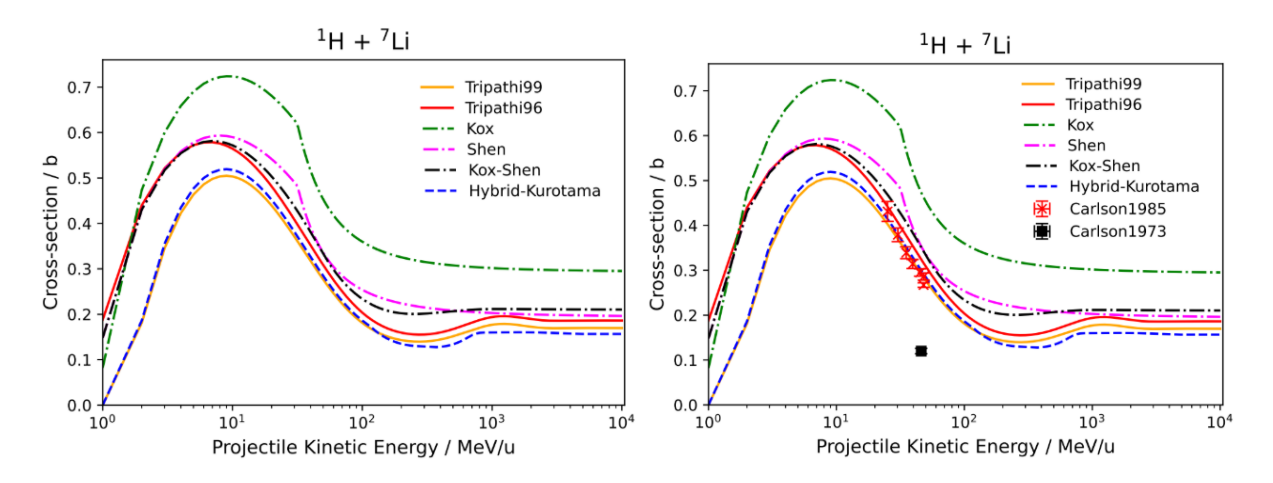


Figure 5: Comparison between models results and cross-section data for proton projectiles on ⁷Li targets, before (Fig. 5a) and after (Fig. 5b) the addition to the database of proton-projectile data presented in this work. IK stands for inverse kinematic data.

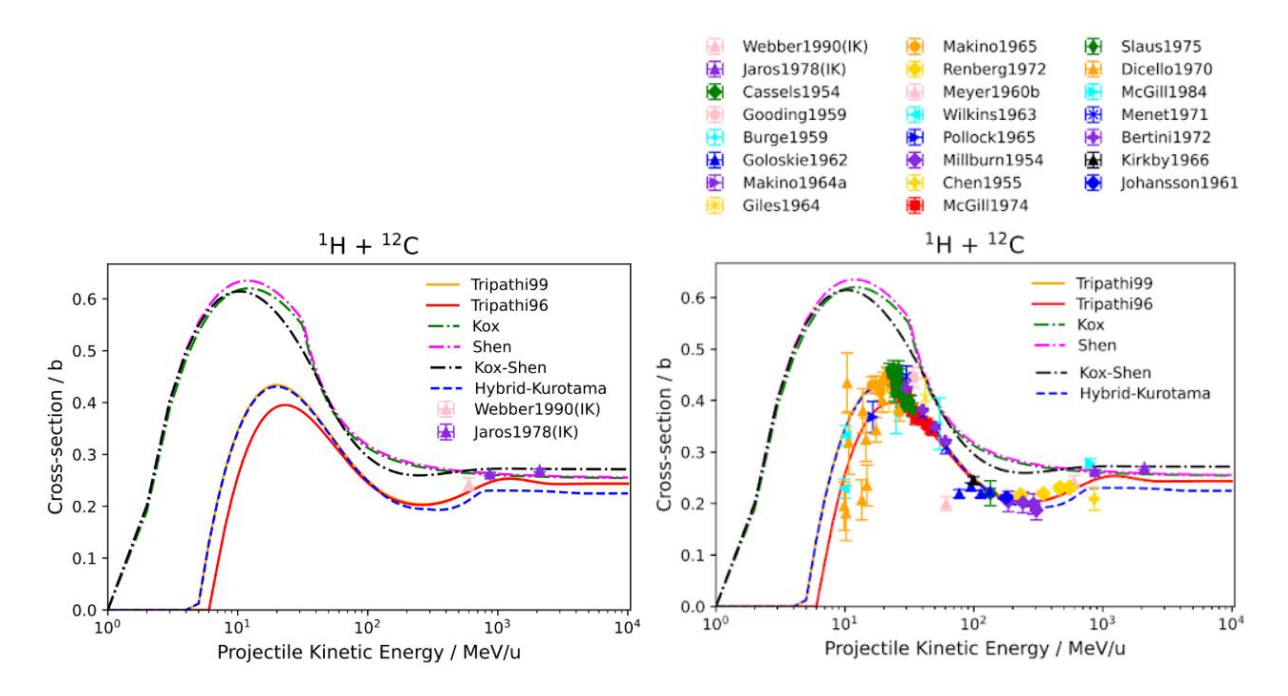


Figure 6: Comparison between models results and cross-section data for proton projectiles on ¹²C targets, before (Fig. 6a) and after (Fig. 6b) the addition to the database of proton-projectile data presented in this work. IK stands for inverse kinematic data.

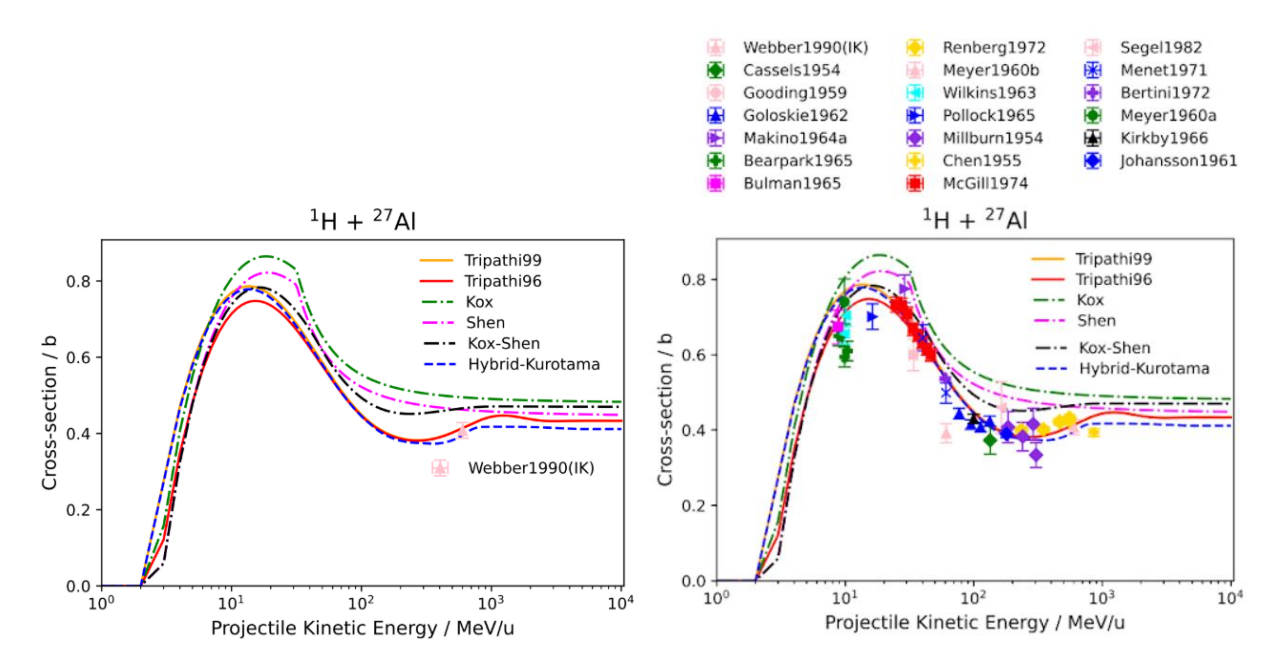


Figure 7: Comparison between models results and cross-section data for proton projectiles on ²⁷Al targets, before (Fig. 7a) and after (Fig. 7b) the addition to the database of proton-projectile data presented in this work. IK stands for inverse kinematic data.

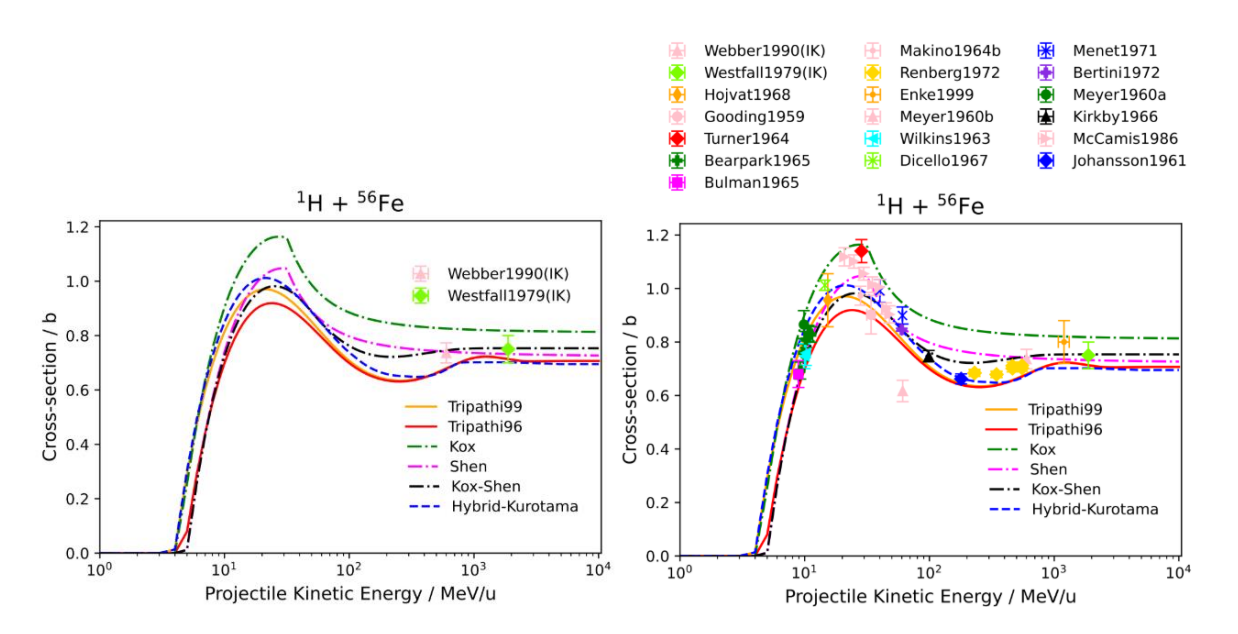


Figure 8: Comparison between models results and cross-section data for proton projectiles on ⁵⁶Fe targets, before (Fig. 8a) and after (Fig. 8b) the addition to the database of proton-projectile data presented in this work. IK stands for inverse kinematic data.

3. Conclusions

Precise nuclear cross-section measurements are needed for the radiation transport codes used for ion-therapy and space radiation protection applications. Therefore, a nucleus-nucleus reaction cross-section database was generated within a GSI-ESA-NASA collaboration (Luoni et al. (2021)). The collected nucleus-nucleus reaction cross-section data were compared with several nuclear reaction cross-section models implemented in the radiation transport codes used for radiation protection in space and ion-therapy applications, namely the Kox, Shen, Kox-Shen, Tripathi-Cucinotta-Wilson (Tripathi99 for low-Z projectile ions and Tripathi96 for the others), and Hybrid-Kurotama models. As a consequence, the Tripathi-Cucinotta-Wilson model was optimized to better fit all of the collected reaction cross-section data (Luoni et al. (2023)).

Although proton-projectile data were not included in the original database, protons are the main contributors to SEP and GCR fluences in space, accounting for most of the effective dose behind thick shields. Furthermore, protons are the ion beam used in 88% of the cancer-treatment ion-therapy centers worldwide. Proton-projectile data can also be used in inverse kinematics, as ¹H is also an important target for both space radiation and ion-therapy endpoints. Therefore, in this work, the addition of proton-projectile data to the reaction database is presented. The addition of these data facilitates the comparison of the reaction cross-section models to a larger dataset. The Tripathi99 and the Hybrid-Kurotama model, which superimposes with Tripathi99 at low energies, are shown to best reproduce the reaction cross-sections for proton-nucleus collisions.

The database can be can be found in the free and open-access web application on the GSI official website⁸. The database provides the scientific community with a comprehensive and detailed set of data for benchmarking nuclear reaction models or for other endpoints, including heavy-ion-therapy with innovative (Tessonnier et al. (2023), Sokol et al. (2017), Mizushima et al. (2019)) and radioactive beams (Mohammadi et al. (2019), Boscolo et al. (2021), Horst et al. (2021)), nuclear and accelerator engineering, nuclear physics and astrophysics (Norbury et al. (2012)).

Acknowledgements

The work was supported in the framework of work package 200 of the ROSSINI3 project (ESA Contract No.4000125785/18/NL/GLC), which was a 2-year project initiated in December 2018, funded by ESA ESTEC and led by Thales Alenia Space Italia. The GET_INvolved Erasmus+ Program at FAIR and GSI (Reference: GI-221246S-HU-STE) generously funded the addition of proton data work. The NASA Research Contract 80LARC23DA003 also supported this work.

⁸ https://www.gsi.de/fragmentation

The authors acknowledge Dr. Robert Reedy and Dr. Felix Horst for providing further details about the data reported in their publications and useful references.

References

Abegg R, Birchall J, Davison N, Dejong M, Ginther D, Hasell D, Nasr T, vanOers W, Carlson R, Cox A. Measurement of the proton total reaction cross section for ¹⁵⁹Tb, ¹⁸¹Ta and ¹⁹⁷Au between 20 and 48 MeV. Nucl Phys A 324:109-114; 1979.

Afshinnekoo E, Scott RT, Matthew FM, Pariset E, Cekanaviciute E, Barker R, Gilroy S, Hassane D, Smith SM, Zwart SR, Nelman-Gonzalez M, Crucian BE, Ponomarev SA,Orlov OI, Shiba D, Muratani M, Yamamoto M, Richards SE, Vaishampayan PA, Meydan C, Foox J, Myrrhe J, Istasse E, Singh N, Venkateswaran K, Keune JA, Ray HE, Basner M, Miller J, Vitaterna MH, Taylor DM, Wallace D, Rubins K, Bailey SM, Grabham P, Costes SV, Mason CE, Beheshti A, Fundamental Biological Features of Spaceflight: Advancing the Field to Enable Deep-Space Exploration. Cell 183:1162-1184; 2020.

Agostinelli S, Allison J, Amako K, Apostolakis J, Araujo H, Arce P, Asai M, Axen D, Banerjee S, Barrand G, Behner F, Bellagamba L, Boudreau J, Broglia L, Brunengo A, Burkhardt H, Chauvie S, Chuma J, Chytracek R, Cooperman G, Cosmo G, Degtyarenko P, DellAcqua A, Depaola G, Dietrich D, Enami R, Feliciello A, Ferguson C, Fesefeldt H, Folger G, Foppiano F, Forti A, Garelli S, Giani S, Giannitrapani R, Gibin D, Gomez Cadenas JJ, Gonzalez I, Gracia-Abril G, Greeniaus G, Greiner W, Grichine V, Grossheim A, Guatelli S, Gumplinger P, Hamatsu R, Hashimoto K, Hasui H, Heikkinen A, Howard A, Ivanchenko V, Johnson A, Jones FW, Kallenbach J, Kanaya N, Kawabata M, Kawabata Y, Kawaguti M, Kelner S, Kent P, Kimura A, Kodama T, Kokoulin R, Kossov M, Kurashige H, Lamanna E, Lampen T, Lara V, Lefebure V, Lei F, Liendl M, Lockman W, Longo F, Magni S, Maire M, Medernach E, Minamimoto K, MoradeFreitas P, Morita Y, Murakami K, Nagamatu M, Nartallo R, Nieminen P, Nishimura T, Ohtsubo K, Okamura M, Oneale S, Oohata Y, Paech K, Perl J, Pfeiffer A, Pia MG, Ranjard F, Rybin A, Sadilov S, DiSalvo E, Santin G, Sasaki T, Savvas N, Sawada Y, Scherer S, Sei S, Sirotenko V, Smith D, Starkov N, Stoecker H, Sulkimo J, Takahata M, Tanaka S, Tcherniaev E, Safai-Tehrani E, Tropeano M, Truscott P, Uno H, Urban L, Urban P, Verderi M, Walkden A, Wander W, Weber H, Wellisch JP, Wenaus T, Williams DC, Wright D, Yamada T, Yoshida H, Zschiesche D. Geant4—a simulation toolkit. Nucl Instrum Methods Phys Res A 506(3):250-303; 2003.

Albert RD, Hansen LF. 10-Mev Proton Reaction Cross Sections for ⁶³Cu and ⁶⁵Cu. Phys Rev Lett 6:13-14; 1961.

Allison J, Amako K, Apostolakis J, Arce P, Asai M, Aso T, Bagli E, Bagulya A, Banerjee S, Barrand G, Beck BR, Bogdanov AG, Brandt D, Brown JMC, Burkhardt H, Canal Ph, Cano-Ott D, Chauvie S, Cho K, Cirrone GAP, Cooperman G, Cortes-Giraldo MA, Cosmo G, Cuttone G, Depaola G, Desorgher L, Dong X, Dotti A, Elvira VD, Folger G, Francis Z, Galoyan A, Garnier L, Gayer M, Genser KL, Grichine VM, Guatelli S, Gueye P, Gumplinger P, Howard AS, Hrivnacova I, Hwang S, Incerti S, Ivanchenko A, Ivanchenko VN, Jones FW, Jun SY, Kaitaniemi P, Karakatsanis N, Karamitros M, Kelsey M, Kimura A, Koi T, Kurashige H, Lechner A, Lee SB, Longo F, Maire M, Mancusi D, Mantero A, Mendoza E, Morgan B, Murakami K, Nikitina T, Pandola L, Paprocki P, Perl J, Petrovic I, Pia MG, Pokorski W, Quesada JM, Raine M, Reis MA, Ribon A, Ristic-Fira A, Romano F, Russo G, Santin G, Sasaki T, Sawkey D, Shin JI, Strakovsky II, Taborda A, Tanaka S, Tome B, Toshito T, Tran HN, Truscott PR, Urban L,

Uzhinsky V, Verbeke JM, Verderi M, Wendt BL, Wenzel H, Wright DH, Wright DM, Yamashita T, Yarba J, Yoshida H. Recent developments in Geant4. Nucl Instrum Methods Phys Res A 835:186-225; 2016.

Anderson BD, Bevington PR, Cverna FH, McNaughton MW, Willard HB, Barrett RJ, King NSP, Ernst DJ. Proton total reaction cross section measurements for ^{40,44,48}Ca at 700 MeV. Phys Rev C 19:905-912; 1979.

Battistoni G, Boehlen T, Cerutti F, Chin PW, Esposito LS, Fasso A, Ferrari A, Lechner A, Empl A, Mairani A, Mereghetti A, Garcia Ortega P, Ranft J, Roesler S, Sala PR, Vlachoudis V, Smirnov G. Overview of the FLUKA code. Ann Nucl Energy 82:10-18; 2015.

Bearpark K, Graham WR, Jones G. Total proton and deutron reaction cross-sections in the energy range 8.5 to 11.5 MeV. Nucl Phys 73:206-216; 1965.

Bellinzona EV, Grzanka L, Attili A, Tommasino F, Friedrich T, Kramer M, Scholz M, Battistoni G, Embriaco A, Chiappara D, Cirrone GAP, Petringa G, Durante M, Scifoni E. Biological Impact of Target Fragments on Proton Treatment Plans: An Analysis Based on the Current Cross-Section Data and a Full Mixed Field Approach. Cancers 13:4768; 2021.

Benton ER, Benton EV. Space radiation dosimetry in low-Earth orbit and beyond. Nucl Instrum Methods Phys Res B.184: 255-94; 2001.

Bertini HW. Reaction Cross Sections for 30- to 60-MeV Protons on Various Elements: Comparison of Theoretical Results with Experiment. Phys Rev C 5:2118-2119; 1972.

Bertrand FE, Peelle RW. Complete Hydrogen and Helium Particle Spectra from 30- to 60-MeV Proton Bombardment of Nuclei with A=12 to 209 and Comparison with the Intranuclear Cascade Model. Phys Rev C 8:1045-1064; 1973.

Boscolo D, Kostyleva D, Safari MJ, Anagnostatou V, Aeystoe J, Bagchi S, Binder T, Dedes G, Dendooven P, Dickel T, Drozd V, Franczack B, Geissel H, Gianoli C, Graeff C, Grahn T, Greiner F, Haettner E, Haghani R, Harakeh MN, Horst F, Hornung C, Hucka JP, Kalantar-Nayestanaki N, Kazantseva E, Kindler B, Knoebel R, Kuzminchuk-Feuerstein N, Lommel B, Mukha I, Nociforo C, Ishikawa S, Lovatti G, Nitta M, Ozoemelam I, Pietri S, Wolfgang RP, Prochazka A, Purushothaman S, Reidel CA, Roesch H, Schirru F, Schuy C, Sokol O, Steinsberger T, Tanaka YK, Tanihata I, Thirolf P, Tinganelli W, Voss B, Weber U, Weick H, Winfield JS, Winkler M, Zhao J, Scheidenberger C, Parodi K, Durante M. Radioactive Beams for Image-Guided Particle Therapy: The BARB Experiment at GSI. Front Oncol 11:737050; 2021.

Brechtmann C, Heinrich W. Measurements of elemental fragmentation cross section for relativistic heavy ions using CR39 plastic nuclear track detectors. Nucl Instrum Methods Phys Res B 29:675-679; 1988.

Brechtmann C, Heinrich W, Benton EV. Fragmentation cross sections of ²⁸Si at 14.5 GeV/nucleon. Phys Rev C 39:2222-2226; 1989.

Bulman PJ, Greenlees GW, Sametband MJ. Proton reaction cross sections at 8.8 MeV. Nucl Phys 69:536-544; 1965.

Bulman PJ, Griffith JAR. Proton total reaction cross sections at 9.1 MeV. Nucl Phys A 111:315-320; 1968.

Burge EJ. The total proton reaction cross section of carbon from 10-68 MeV by a new method. Nucl Phys 13:511-515; 1959.

Carlson RF, Cox AJ, Nasr TN, De Jong MS, Ginther DL, Hasell DK, Sourkes AM, vanOers WTH, Margaziotis DJ. Measurements of proton total reaction cross sections for ⁶Li, ⁷Li, ¹⁴N, ²⁰N and ⁴⁰Ar between 23 and 49 MeV. Nucl Phys A 445:57-69; 1985.

Carlson RF, Doherty P, Margaziotis DJ, Slaus I, Tin SY, vanOers WTH. Proton-deuteron total reaction cross-sections in the energy range (20÷50) MeV. Lett Nuovo Cimento 8:319-323; 1973.

Carlson RF, Eisberg RM, Stokes RH, Short TH. Total proton reaction cross section of copper at 9 MeV. Nucl Phys 36:511-516; 1962.

Carlson RF, Cox AJ, Nimmo JR, Davison NE, Elbakr SA, Horton JL, Houdayer A, Sourkes AM, vanOers WTH, Margaziotis DJ. Proton total reaction cross sections for the doubly magic nuclei ¹⁶O, ⁴⁰Ca, and ²⁰⁸Pb in the energy range 20-50 MeV. Phys Rev C 12:1167-1175; 1975.

Carlson RF, Cox AJ, Davison NE, Eliyakut-Roshko T, McCamis RH, vanOers WTH. Proton total reaction cross sections for ⁴²Ca, ⁴⁴Ca, and ⁴⁸Ca between 21 and 48 MeV. Phys Rev C:3090-3037; 1994.

Carlson RF, Cox AJ, Eliyakut-Roshko T, vanOers WTH. Measurements of proton total reaction cross sections for ^{112,114,116,118,120,122,124}Sn from 22 to 48 MeV. Can J Chem 73:512-518; 1995.

Cassels JM, Lawson JD. Absorption Cross Sections for 134 MeV Protons. Proc Phys Soc A 67:125-133; 1954.

Cecchini S, Chiarusi T, Giacomelli G, Giorgini M, Kumar A, Mandrioli G, Manzoor S, Margiotta AR, Medinaceli E, Patrizii L, Popa V, Qureshi IE, Sirri G, Spurio M, Togo V. Fragmentation cross sections of ⁵⁶Fe, ¹⁴Si and ⁶C ions of 0.3-10 AGeV on polyethylene, CR39 and aluminum targets. Nucl Phys A 807:206-213; 2008.

Chancellor JC, Scott GBI, Sutton JP. Space Radiation: The Number One Risk to Astronaut Health beyond Low Earth Orbit. Life 4:491-510; 2014.

Chapman R, Macleod AM. Proton nuclear reaction cross sections in oxygen and neon at 13 MeV. Nucl Phys A 94:313-323; 1967.

Chen FF, Leavitt CP, Shapiro AM. Attenuation Cross Sections for 860-Mev Protons. Phys Rev 99:857-871; 1955.

Davison NE, Hasell DK, Sourkes AM, vanOers WTH, Carlson RF, Cox AJ, Margaziotis DJ. Measurements of the proton total reaction cross section for ²⁴Mg, ^{64,66,68}Zn and ¹⁴⁰Ce between 17.5 and 48 MeV. Nucl Phys A 290:45-54; 1977.

Dell GF, Ploughe WD, Hausman HJ. Total reaction cross sections in the mass range 45 to 65. Nucl Phys 64:513-523; 1965.

Dicello JF, Igo G. Proton Total Reaction Cross Sections in the 10-20-MeV Range: Calcium-40 and Carbon-12. Phys Rev C 2:488-499; 1970.

Dicello JF, Igo GJ, Roush ML. Proton Total Reaction Cross Sections for 22 Isotopes of Ti, Fe, Ni, Cu, Zn, Zr, and Sn at 14.5 MeV. Phys Rev 157:1001-1015; 1967.

Durante M, Haberer T. Twenty-Five Years of Carbon Ion Radiotherapy in Europe. Nucl Phys News 34:21-24; 2024.

Durante M, Paganetti H. Nuclear physics in particle therapy: a review. Rep Prog Phys 79:096702; 2016.

Eliyakut-Roshko T, McCamis RH, vanOers WTH, Carlson RF, Cox AJ. Measurements of proton total reaction cross sections for ⁵⁸Ni and ⁶⁰Ni including non relativistic and relativistic data analyses. Phys Rev C 51:1295-1302; 1995.

Enke M, Herbach CM, Hilscher D, Jahnke U, Schapiro O, Letourneau A, Galin J, Goldenbaum F, Lott B, Peghaire A, Filges D, Neef RD, Nunighoff K, Paul N, Schaal H, Sterzenbach G, Tietze A, Pienkowski L. Evolution of a spallation reaction: experiment and Monte Carlo simulation. Nucl Phys A 657:317-339; 1999.

Ferrando P, Webber WR, Goret P, Kish JC, Schrier DA, Soutoul A, Testard O. Measurement of ¹²C, ¹⁶O, and ⁵⁶Fe charge changing cross sections in helium at high energy, comparison with cross sections in hydrogen, and application to cosmic-ray propagation. Phys Rev C 37:1490-1501; 1988.

Giles RA, Burge EJ. The measurement of the total proton reaction cross-section of carbon in the energy region up to 50 MeV. Nucl Phys 50:327-336; 1964.

Goloskie R, Strauch K. Measurement of proton inelastic cross sections between 77 MeV and 133 MeV. Nucl Phys 29:474-485; 1962.

Gooding TJ. Proton total reaction cross sections at 34 MeV. Nucl Phys 12:241-248; 1959.

Greenlees GW, Jarvis ON. A Direct Measurement of the Proton Total Reaction Cross Section for Copper at 9.3 Mev. Proc Phys Soc 78:1275-1284; 1961.

Hirzebruch SE, Heinrich W, Tolstov KD, Kovalenko AD, Benton EV. Fragmentation cross sections of ¹⁶O between 0.9 and 200 GeV/nucleon. Phys Rev C 46:1487-1494; 1992.

Hojvat C, Jones G. An associated particle method for measuring total proton reaction cross sections at 15.8 MeV. Nucl Instrum Methods 66:13-24; 1968.

Horst F, Arico G, Brinkmann KT, Brons St, Ferrari A, Haberer T, Mairani A, Parodi K, Reidel CA, Weber U, Zink K, Schuy C. Measurement of ⁴He charge- and mass-changing cross sections on H, C, O, and Si targets in the energy range 70–220 MeV/u for radiation transport calculations in ion-beam therapy. Phys Rev C 99:014603; 2019.

Horst F, Schardt D, Iwase H, Schuy C, Durante M, Weber U. Physical characterization of ³He ion beams for radiotherapy and comparison with ⁴He. Phys Med Biol 66:095009; 2021.

Hugo G, Ahdida C, Bozzato D, Calzolari D, Cerutti F, Ciccotelli A, Cimmino A, Devienne A, Donadon Servelle A, Dyrcz PK, Esposito LS, Formento A, Froeschl R, Garcia Alia R, Gilardoni S, Gomes A, Horváth D, Humann B, Infantino A, Lechner A, Lefebvre B, Lerner G, Lorenzon T, Lucsanyi D, Magistris M, Marin S, Mazzola G, Niang S, Nowak E, Ogallar Ruiz F, Potoine JB, Pozzi F, Prelipcean D, Rodin V, Roesler S, Sabate Gilarte M, Sacristan Barbero M, Salvat Pujol F, Schoofs P, Serban AG, Sharankov I, Theis C, Tisi M, Tsinganis A, Versaci R, Vlachoudis V, Waets A, Widorski M, Zymak I. Latest FLUKA Developments. EPJ N 10:20; 2024.

Jaros J, Wagner A, Anderson L, Chamberlain O, Fuzesy RZ, Gallup J, Gorn W, Schroeder L, Shannon S, Shapiro G, Steiner H. Nucleus-nucleus total cross sections for light nuclei at 1.55 and 2.89 GeV per nucleon. Phys Rev C 18:2273-2292; 1978.

Johansson A, Svanberg U, Sundberg O. Total Nuclear Reaction Cross Sections For 180 MeV Protons. Arkiv Fysik 19; 1961.

Kirkby P, Link WT. Faraday-cup Measurement of Proton Total Reaction Cross Sections at 100 MeV. Can J Phys 44:1847-1862; 1966.

Koontz SL, Boeder PA, Pankop C, Reddell B. The ionizing radiation environment on the International Space Station: performance vs. expectations for avionics and materials. IEEE Radiation Effects Data Workshop:110-116; 2005.

Kox S, Gamp A, Perrin C, Arvieux J, Bertholet R, Bruandet JF, Buenerd M, Cherkaoui R, Cole AJ, El-Masri Y, Longequeue N, Menet J, Merchez F, Viano JB. Trends of total reaction cross sections for heavy ion collisions in the intermediate energy range. Phys Rev C 35:1678-1691; 1987.

Kraemer M, Jaekel O, Haberer T, Kraft G, Schardt D, Weber U. Treatment planning for heavy-ion radiotherapy: physical beam model and dose optimization. Phys Med Biol 45:3299-317; 2000.

Luoni F. Radiation Shielding during Deep-Space Missions: Dose Measurements, Monte Carlo Simulations, and Nuclear Cross-Sections. Technical University of Darmstadt; 2023. Thesis.

Luoni F, Boscolo D, Fiore G, Bocchini L, Horst F, Reidel CA, Schuy C, Cipriani C, Binello A, Baricco M, Giraudo M, Santin G, Durante M, Weber U. Dose attenuation in innovative shielding materials for radiation protection in space: measurements and simulations. Radiat Res 198:107-119; 2022.

Luoni F, Horst F, Reidel CA, Quarz A, Bagnale L, Sihver L, Weber U, Norman RB, deWet W, Giraudo M, Santin G, Norbury JW, Durante M. Total nuclear reaction cross-section database for radiation protection in space and heavy-ion therapy applications. New J Phys 23:101201; 2021.

Luoni F, Reidel CA, Horst F, Weber U, Durante M. Optimisation of the Tripathi model using a nuclear reaction cross-section database. New J Phys 25:123024; 2023.

Luoni F, Weber U, Alica KL, Westermayer M, Horst F, Baricco M, Bocchini GM, Santin G, Schuy C, Durante M, Boscolo D. Dose Build-up of High-energy ¹H and ⁴He Ions in Standard, Innovative and In Situ Shielding Materials for Space Radiation: Measurements and Simulations. Rad Res 203:163-174; 2025.

Makino MQ, Waddell CN, Eisberg RM. Total reaction cross sections for 29 MeV protons. Nucl Phys 50:145-156; 1964a.

Makino MQ, Waddell CN, Eisberg RM. Proton total reaction cross sections of carbon from 16 to 28 MeV. Nucl Phys 68:378-386; 1965.

Makino MQ, Waddell CN, Eisberg RM, Hestenes J. Study of shell closure effect on proton total reaction cross sections. Phys Lett 9:178-180; 1964b.

McCamis RH, Davison NE, vanOers WTH, Carlson RF, Cox AJ. A study of proton total reaction cross sections for several medium-mass nuclei between 20 and 48 MeV. Can J Phys 64:685-691; 1986.

McGill WF, Carlson RF, Short TH, Cameron JM, Richardson JR, Slaus I, vanOers WTH, Verba JW, Margaziotis DJ, Doherty P. Measurements of the proton total reaction cross section for light nuclei between 20 and 48 MeV. Phys Rev C 10:2237-2246; 1974.

McGill JA, Hoffmann GW, Barlett ML, Fergerson RW, Milner EC, Chrien RE, Sutter RJ, Kozlowski T, Stearns RL. Proton + nucleus inclusive (p,p') scattering at 800 MeV. Phys Rev C 29:204-208; 1984.

Menet JJH, Gross EE, Malanify JJ, Zucker A. Total-Reaction-Cross-Section Measurements for 30-60-MeV Protons and the Imaginary Optical Potential. Phys Rev C 4:1114-1129; 1971.

Meyer V, Hintz NM. Charged Particle and Total Reaction Cross Sections for Protons at 9.85 Mev. Phys Rev Lett 5:207-209; 1960a.

Meyer V, Eisberg RM, Carlson RF. Total Reaction Cross Sections of Several Nuclei for 61-Mey Protons. Phys Rev 117:1334-1336; 1960b.

Millburn GP, Birnbaum W, Crandall WE, Schecter L. Nuclear Radii from Inelastic Cross-Section Measurements. Phys Rev 95:1268-1278; 1954.

Mizushima K, Furukawa T, Iwata Y, Muramatsu M, Sato S, Hara Y, Tansho R, Saraya Y, Saotome N, Shirai T, Noda K. Experimental verification of beam switching operation for

multiple-ion therapy applications at HIMAC. Nucl Instrum Methods Phys Res B 459:115-119; 2019.

Mohammadi A, Tashima H, Iwao Y, Takyu S, Akamatsu G, Nishikido F, Yoshida E, Kitagawa A, Parodi K, Yamaya T. Range verification of radioactive ion beams of ¹¹C and ¹⁵O using inbeam PET imaging. Phys Med Biol 64:145014; 2019.

Mohan R, Grosshans D. Proton therapy - Present and future. Adv Drug Deliv Rev. 109:26-44; 2017.

Montague DG, Cole RK, Makino M, Waddell CN. Proton total reaction cross sections of Beryllium from 16 to 28 MeV. Nucl Phys A 199:457-462; 1973.

Nasr TN, Sourkes AM, Margaziotis DJ, Carlson RF, Cox AJ. Measurements of the total reaction cross section for protons on Ti and B between 20 and 50 MeV. Can J Phys 56:56-62; 1978.

National Academies/National Research Council. Managing Space Radiation Risk in the New Era of Space Exploration. Washington, DC: The National Academies Press; 2008.

Neumaier SR, Alkhazov GD, Andronenko MN, Dobrovolsky AV, Egelhof P, Gavrilov GE, Geissel H, Irnich H, Khanzadeev AV, Korolev GA, Lobodenko AA, Munzenberg G, Mutterer M, Schwab W, Seliverstov DM, Suzuki T, Timofeev NA, Vorobyov AA, Yatsoura VI. Small-angle proton elastic scattering from the neutron-rich isotopes ⁶He and ⁸He, and from ⁴He, at 0.7 GeV in inverse kinematics. Nucl Phys A 712:247-268; 2002.

Nicholls JE, Craig A, Griffith TC, Imrie DC, Lush CJ, Metheringham AJ. Inelastic p-⁴He scattering at 141 MeV. Nucl Phys A 181:329-336; 1972.

Norbury JW, Battistoni G, Besuglow J, Bocchini L, Boscolo D, Botvina A, Clowdsley M, deWet W, Durante M, Giraudo M, Haberer T, Heilbronn L, Horst F, Kramer M, LaTessa C, Luoni F, Mairani A, Muraro S, Norman RB, Patera V, Santin G, Schuy C, Sihver L, Slaba TC, Sobolevsky N, Topi A, Weber U, Werneth CM, Zeitlin CJ. Are Further Cross Section Measurements Necessary for Space Radiation Protection or Ion Therapy Applications? Helium Projectiles. Front Phys 8:409; 2020.

Norbury JW, Miller J, Adamczyk AM, Heilbronn LH, Townsend LW, Blattnig SR, Norman RB, Guetersloh SB, Zeitlin CJ. Nuclear data for space radiation. Radiat Meas 47:315-363; 2012.

Norbury JW, Miller J, Adamczyk AM, Heilbronn LH, Townsend LW, Blattnig SR, Norman RB, Guetersloh SB, Zeitlin CJ. Review of nuclear physics experiments for space radiation. Radiat Meas 47:315; 2011.

Pollock RE, Schrank G. Proton Total Reaction Cross Sections at 16.4 MeV. Phys Rev 140:B575-B585; 1965.

Renberg PU, Measday DF, Pepin M, Schwaller P, Favier B, Richard-Serre C. Reaction cross sections for protons in the energy range 220–570 MeV. Nucl Phys A 183:81-104; 1972.

Segel RE, Chen T, Rutledge LL, Maher JV, Wiggins J, Singh PP, Debevec PT. Inclusive proton reactions at 164 MeV. Phys Rev C 26:2424-2432; 1982.

Shen WQ, Wang B, Feng J, Zhan WI, Zhu YT, Feng EP. Total reaction cross section for heavy-ion collisions and its relation to the neutron excess degree of freedom. Nucl Phys A 491:130-146; 1989.

Sihver L, Kohama A, Iida K, Oyamatsu K, Hashimoto S, Iwase H, Niita K. Current status of the "Hybrid Kurotama model" for total reaction cross-sections. Nucl Instrum Methods Phys Res B 334:34-39; 2014a.

Sihver L, Lantz M, Kohama A. Improved parametrization of the transparency parameter in Kox and Shen models of total reaction cross-sections. Phys Rev C 89:067602; 2014b.

Singh BK, Ojha ID, Tuli SK. Some general characteristics of ²⁸Si-emulsion interactions at 4.5 GeV/c per nucleon. Nucl Phys A 570:819-832; 1994.

Slaba TC, Blattnig SR, Reddell B, Bahadori A, Norman RB, Badavi FF. Pion and electromagnetic contribution to dose: Comparisons of HZETRN to Monte Carlo results and ISS data. Adv Space Res 52:62-78; 2013.

Slaba TC, Blattnig SR. GCR environmental models I: Sensitivity analysis for GCR environments. Space Weather 12:217-224; 2014.

Slaba TC, Bahadori AA, Reddell BD, Singleterry RC, Clowdsley MS, Blattnig SR. Optimal shielding thickness for galactic cosmic ray environments. Life Sci Space Res 12:1-15; 2017.

Slaba TC, Wilson JW, Werneth CM, Whitman K. Updated deterministic radiation transport for future deep space missions. Life Sci Space Res 27:6-18; 2020.

Slaus I, Margaziotis DJ, Carlson RF, vanOers WTH, Richardson JR. Structure in the energy dependence of the proton total reaction cross section for C and Si in the energy region 20-40 MeV. Phys Rev C 12:1093-1095; 1975.

Sokol O, Scifoni E, Tinganelli W, Kraft-Weyrather W, Wiedemann J, Maier A, Boscolo D, Friedrich T, Brons S, Durante M, Kramer M. Oxygen beams for therapy: advanced biological treatment planning and experimental verification. Phys Med Biol 62:7798-7813; 2017.

Sourkes AM, Houdayer A, vanOers WTH, Carlson RF, Ronald EB. Total reaction cross section for protons on ³He and ⁴He between 18 and 48 MeV. Phys Rev C 13:451-460; 1976.

Szabo R. Nuclear Reaction and Fragment Production Cross-Section Database for Space and Heavy-Ion Therapy Applications: Proton Data. GSI FAIR: GI-221246S-HU-STE; 2023. Available at https://edms.cern.ch/document/3237253/1.

Tessonnier T, Ecker S, Besuglow J, Naumann J, Mein S, Longarino FK, Ellerbrock M, Ackermann B, Winter M, Brons S, Qubala A, Haberer T, Debus J, Jaekel O, Mairani A. Commissioning of Helium Ion Therapy and the First Patient Treatment With Active Beam Delivery. Int J Radiat Oncol Biol Phys 116:935-948; 2023.

Tinganelli W, Luoni F, Durante M. What can space radiation protection learn from radiation oncology?. Life Sci Space Res 30:82-95; 2021.

Townsend LW, Cucinotta FA, Heilbronn LH. Nuclear model calculations and their role in space radiation research. Adv Space Res 30:907-916; 2002.

Tripathi R, Cucinotta F, Wilson J. Accurate universal parameterization of absorption cross sections. Nucl. Instrum. Methods Phys Res B 117:347-349; 1996.

Tripathi R, Cucinotta F, Wilson J. Accurate universal parameterization of absorption cross sections III – light systems. Nucl Instrum Methods Phys Res B 155:349-356; 1999.

Turner JF, Ridley BW, Cavanagh PE, Gard GA, Hardacre AG. Optical model studies of proton scattering at 30 MeV. Nucl Phys 58:509-514; 1964.

Washburn SA, Blattnig SR, Singleterry RC, Westover SC. Active magnetic radiation shielding system analysis and key technologies. Life Sci Space Res 4:22-34; 2015.

Webber WR, Kish JC, Schrier DA. Total charge and mass changing cross sections of relativistic nuclei in hydrogen, helium, and carbon targets. Phys Rev C 41:520-532; 1990.

Webber WR, Kish JC, Rockstroh JM, Cassagnou Y, Legrain R, Soutoul A, Testard O, Tul Cl. Production Cross Sections of Fragments from Beams of 400-650 MeV per Nucleon ⁹Be, ¹¹B, ¹²C, ¹⁴N, ¹⁵N, ¹⁶O, ²⁰Ne, ²²Ne, ⁵⁶Fe, and ⁸Ni Nuclei Interacting in a Liquid Hydrogen Target. I. Charge Changing and Total Cross Sections. ApJ 508:940-948; 1998a.

Webber WR, Soutoul A, Kish JC, Rockstroh JM, Cassagnou Y, Legrain R, Soutoul A, Testard O. Measurement of charge changing and isotopic cross sections at ~600 MeV/nucleon from the interactions of ~30 separate beams of relativistic nuclei from ¹⁰B to ⁵⁵Mn in a liquid hydrogen target. Phys Rev C 58:3539-3552; 1998b.

Westfall GD, Wilson LW, Lindstrom PJ, Crawford HJ, Greiner DE, Heckman HH. Fragmentation of relativistic ⁵⁶Fe. Phys Rev C 19:1309-1323; 1979.

Wilkins BD, Igo G. 10-MeV Proton Reaction Cross Sections for Several Elements. Phys Rev 129:2198-2206; 1963.

Zeitlin C, Fukumura A, Guetersloh SB, Heilbronn LH, Iwata Y, Miller J, Murakami T. Fragmentation cross sections of ²⁸Si at beam energies from 290 A to 1200 AMeV. Nucl Phys A 784:341-367; 2007a.

Zeitlin C, Guetersloh S, Heilbronn L, Miller J, Fukumura A, Iwata Y, Murakami T. Fragmentation cross sections of 290 and 400 MeV/nucleon ¹²C beams on elemental targets. Phys Rev C 76:014911; 2007b.

Zeitlin C, Miller J, Guetersloh S, Heilbronn L, Fukumura A, Iwata Y, Murakami T, Blattnig S, Norman R, Mashnik S. Fragmentation of ¹⁴N, ¹⁶O, ²⁰Ne, and ²⁴Mg nuclei at 290 to 1000 MeV/nucleon. Phys Rev C 83:034909; 2011.